A POSSIBLE EXPLANATION OF CONCRETE POP-OUTS

by

J. H. Havens and R. C. Deen

ABSTRACT

This report summarizes several years of research relating to damage to concrete and aggregates undergoing freezing and thawing. Basic principles involving freezing and attendant pressures are considered. Application of these principles to the evaluation of concrete was accomplished in experiments on concrete having low and high air contents.

Freeze-thaw characteristics of saturated aggregates relative to physical properties such as porosity, absorption, and bulk specific gravity were studied by submerging individual particles in pre-chilled mercury. Pressures associated with pop-outs in concrete were monitored and are presented along with accompanying theoretical considerations.

Research Report
460

A POSSIBLE EXPLANATION OF CONCRETE POP-OUTS

BY

J. H. Havens
Director

and

R. C. Deen
Assistant Director

Division of Research
Bureau of Highways
DEPARTMENT OF TRANSPORTATION
Commonwealth of Kentucky

offered for publication to the
Transportation Research Board

December 1976

INTRODUCTION

Voids occur in concrete through the entrapment and entrainment of air, the occlusion of excess mix water, differences in the specific volumes of reactants and hydration products, leaching of hydration products (CaO), and the use of porous aggregates. Those voids which are easily saturated affect durability unfavorably while those which are less permeable are highly favorable to durability. Considerable water is occluded in concrete in the form of excess mix-water and water absorbed by the aggregate. Concrete which has not been allowed to dry following curing and prior to the onset of freezing does not perform as well, in laboratory tests, as concrete which has been dried but otherwise is similar. This indicates that a somewhat irreversible fixation or tightening of the mortar structure attends drying and that the concrete becomes less susceptible to resaturation. In other words, the process of drying may close some of the pores. The use of aggregate which is merely moistened, as opposed to soaked or saturated, in the concrete favorably affects durability -- at least in laboratory freeze-thaw tests. Either or both of these effects may merely be the result of delayed saturation.

Dry concrete is unaffected by the freeze-thaw mechanism. It appears, in fact, that serious damage is sustained only when a high degree of saturation exists. If concrete is relatively impermeable, even though it contains a large percentage of voids, saturation is unlikely to occur unless exposure to water is sustained for a long period of time. In natural exposures, periods of wetting occur alternately with periods of drying; and the durations of drying periods tend to exceed those of wetting periods. In the random courses of nature, a concrete structure such as a bridge would tend to dry; however, long interim periods of wetness followed immediately by freezing may be extremely damaging.

BASIC THERMAL ANALYSIS

The density of water at 32 F (O C) is 62.4 pounds per cubic foot (999.8 kg per m^3); the density of ice at 32 F (O C) is 57.2 pounds per cubic foot (917 kg per m^3) *(1)*. There is an increase in volume of approximately nine percent when water freezes. If water completely fills the pores or voids in concrete and is frozen therein, the concrete must dilate or expand proportionally.

Saturation of all voids to 91.7 percent is termed "critical saturation", alluding to the degree of saturation beyond which the freezing of water overfills the voids with ice and creates internal expansive pressures. While its theoretical meaning is quite clear, its practical meaning as applied to concrete is more in the sense of a statistical average which can be interpreted in two ways: (1) 91.7 percent of

the voids being completely filled or (2) all voids being filled to 91.7 percent of their capacity. The first condition could be extremely damaging to concrete undergoing freezing; if the second possibility accurately described the condition of the water in the concrete, there would be no damage from freezing.

Analogous Phenomena

To demonstrate some basic principles, preliminary experiments were made on rather idealized models *(2)*. First, water in an open vessel was frozen in air, and a time-temperature record was made from a themocouple positioned near the center of the volume. The resulting thermograph, Figure 1, gave a broad step at 32 F (O C) without any noticeable depression of the freezing point. A closed vessel or "steel bomb" was improvised from a 3-inch (76.2-mm) diameter pipe nipple and two cast-iron caps. A valve and thermocouple well were tapped into the nipple. The bomb was filled with water and frozen in air as before, and the resulting thermograph is also shown in Figure 1. Freezing began at 32 F (O C), the freezing point gradually decreased to 25 F (4 C), and then suddenly reverted back to 32 F (O C). The pressure was in close agreement with the estimated ultimate strength of the cast iron caps, 7000 psi (48 MPa).

The ruptured cap was replaced and the bomb filled with water to 96 percent of its capacity. Upon freezing, the thermograph shown in Figure 1 was obtained. Here again, the water began freezing at 32 F (O C), but there was no immediate depression of the freezing point and consequently no immediate build-up of pressure. In this case, development of pressure was delayed until most of the water had frozen. There was only a 6 F (3.3 C) depression of the final freezing point, equivalent to 6200 psi (43 MPa); and, while there was no explosive rupture, the caps yielded considerably under that pressure.

Experimental Phenomena

Figure 2 illustrates a typical time-temperature record obtained from an oven-dried specimen of concrete undergoing one cycle of freeze-thaw. Since the freezing was done in air, the specimen temperature is seen to lag behind the air temperature; and there are no sharp breaks or steps in the cooling curve. Upon flooding the freezing chamber with water at 40 F (4 C), the specimen temperature rose rapidly; but there are no sharp steps or breaks in the curve. In contrast, Figure 2 also illustrates a typical thermograph obtained from highly porous, highly absorptive, highly saturated concrete undergoing a single cycle of freeze-thaw. The steps in the freezing and thawing curves occur at approximately the same temperature, near but not exactly at the normal freezing temperature of water. The portions of the curves above and below that step have characteristically different curvatures, and the steps are not merely off-sets in otherwise normal cooling and heating curves. The slopes of either or both curves as they

approach the step may be described as $\Delta T/\Delta t$, or the incremental change in temperature per increment of time. This factor, when multiplied by the product of the specific heat and weight of the concrete specimen would give the rate at which heat was being removed from the specimen. The product of the time lapse and rate of heat removal should correspond approximately with an isothermal change in heat content (ΔH) accompanying freezing of water in the specimen. From Figure 2, it is also apparent that the freezing step is sloping slightly downward from 32 F (O C), signifying that water began freezing under a normal pressure of 1 atm (98 kPa) but finished freezing at 28 F (15.5 C), which corresponds to the freezing point of pure water under a pressure of approximately 4500 psi (31 MPa). Since there is no apparent depression of the initial freezing point, no supercooling or other interfering mechanism is evident.

A large portion of water absorbed into concrete at saturation may be regarded as being "free" water which is freezable and evaporable in much the same sense that pure water is; and it is this portion of water to which analysis of freezing-point depression and pressure applies most directly. However, a portion of the water, in addition to the water of hydration and crystallization, exists in an infinitely more complex state -- due to internal surface absorption and capillary tensions which abound within the concrete. This portion of water is not expected to exhibit a normal freezing point, and it may be of little or no significance here unless its effects appear as an interfering mechanism distorting the prototype thermograph.

The only other serious possibility of an interfering mechanism is the influence of dissolved electrolytes upon the freezing characteristics of the so-called "free" water. The most abundant solute in hardened concrete is $Ca(OH)_2$; but its solubility at 32 F (O C) is in the order of 1.85 kg per cubic meter of water. Assuming complete saturation and 90-percent dissociation, this would depress the initial freezing point approximately 0.2 F (0.1 C). Since the solution is saturated, it becomes an eutectic or constant-freezing mixture which should otherwise respond to pressure according to the prototype thermograph. The possible effects of alkali available from cement may be similarly estimated by assuming 0.6 percent alkali by weight of cement and the maximum free water to be approximately equal to the excess mix water. This quantity of alkali, if available as solute, would depress the initial freezing point a maximum of 2.5 F (1.4 C). Since no such intial depressions are yet apparent, the concentration of alkali must be rather small, at least while the greater portion of water is freezing. Alkalies such as NaOH and KOH are more or less infinitely soluble in comparison to $Ca(OH)_2$. In dilute solutions of this type, water freezes into ice which is nearly pure and concentrates the salt in the remaining solution; this decreases the freezing point of the remaining solution. This kind of interfering mechanism would cause the freezing point step to curve downward at an increasing rate and there would be no discrete

terminus to the step. A general, but cursory, conception of the effects of pressure and different concentrations of highly soluble electrolytes is illustrated in Figure 3 and are superimposed there upon a normal freezing curve for pure, unrestrained water.

In a subsequent experiment, two sets of 6-inch (152-mm) cubes were cast using a six-bag mix, 3-inch (76-mm) slump, and dense limestone aggregate. In one set 13 percent air was obtained; and 0.7 percent air was obtained in the other set by vibrating the concrete to dispel a good portion of normally entrapped air. The two sets of specimens represent forced extremes in the range of air contents -- as a deliberate attempt to magnify the effects of air content on the thermographs. Three thermocouples were cast into these specimens to further magnify the thermographs. One specimen from each of the two sets was moist cured for 5 weeks prior to beginning of freeze-thaw, and these specimens failed to exhibit any indication of a freezing-point step even after 30 cycles. The companion specimens for each set were cured 14 days and immersed in water for 24 hours prior to beginning freeze-thaw. These specimens exhibited a progressive broadening of the step and a progressive differentiation between the air-entrained concrete and non-air-entrained concretes, indicating the rate of absorption of water by the non-air-entrained concrete was also much greater. Freeze-thaw was continued to 77 cycles, at which time the non-air-entrained specimens were in virtual ruin. Thermographs obtained from the 1st, 40th, and 77th cycles are shown in Figure 4.

Failure of the two concrete specimens which were cured 5 weeks to exhibit a significant thermal step even after 30 cycles of freeze-thaw offers an example of highly retarded or delayed saturation. Continued curing and hydration tends to desiccate smaller interstices of the cement gel and to reduce the "free" water content of the concrete. Continued curing would likewise densify and strengthen the mortar against subsequent ingresses of water. Thus, the mere number of freeze-thaw cycles which a concrete specimen is able to withstand before saturation becomes critical is probably not as significant as the time duration of conditions causing absorption of water and eventual saturation. It is suggested, therefore, that the number of regular cycles or the time preceding development of a significant thermal step and freezing-point depression provides a significant basis for evaluating concrete durability in addition to that of determining the number of cycles producing complete or impending destruction of the concrete.

FREEZE-THAW RESISTANCE OF AGGREGATES

Present test methods of aggregates employ composite samples, and results of such tests provide average values. For example, the average value of absorption obtained from a composite sample may

exhibit a low value -- generally indicating a sound aggregate; however, if each particle were analyzed, it might be found that a portion of the aggregate is so highly absorptive as to be detrimental to concrete. The percentage of these deleterious particles in aggregate is also important. Logically, in determining the soundness of an aggregate sample, the freeze-thaw testing should be conducted on a per-particle basis. Each particle should be saturated at the onset of test and kept saturated during testing. For study purposes, the degree of saturation may be varied. Maximum saturation definitely establishes the ultimate susceptibility of aggregate to damage from freezing and thawing.

Phenomena

To obtain objective data -- definitive relationships between effects of freezing and thawing and the physical properties of porosity, absorption, and bulk specific gravity -- pertaining to the freeze-thaw characteristics of aggregate, a method of test was devised whereby the discrete conditions previously mentioned were fulfilled *(3)*. A freezing medium was sought whereby each aggregate particle could be frozen quickly. The quickly frozen surface would form a seal or shell about the particle and retain the pore water. Also, the medium should not contaminate the pore water. Chilled mercury was chosen as the freezing medium -- it has high thermal conductivity, it is immiscible with water, and it has a low freezing point. The test consisted of submerging the aggregate particle in pre-chilled mercury. From preliminary testing, it was found that if a particle did not show visual distress at the end of four cycles -- which could be performed in a matter of minutes -- it would withstand innumerable cycles.

A saturated gravel, which would represent a variety of rock types and possess a wide range of physical properties, was secured from a glacial outwash deposit and kept inundated to assure saturated conditions. Primary constituents of the aggregate sample were dolomites, cherts, limestones, sandstones, siltstones, and various igneous and metamorphic rock particles. Although usually acceptable for concrete, this gravel contained both sound and unsound particles and provided an assortment of particles needed for study.

After grading according to five sizes ranging from the No. 4 sieve to 1 1/2 inches (33 mm), each particle was numbered. The saturated surface dry weight and bulk volume, by mercury displacement, were obtained for each particle prior to freeze-and-thaw tests. The bulk specific gravity was calculated for each particle. Freezing of the aggregate was accomplished by submerging each particle in cold mercury (-22 to -31 F (-30 to -35 C)) for 5 minutes. The mercury was contained in a glass cylinder enclosed in an insulated container of dry ice (solid CO_2). At the end of each freezing cycle, each particle was removed from the freezing medium and returned to a container of water and allowed to thaw. At the end of each thawing cycle, a visual examination was made of each particle and any distress resulting from the freezing and thawing cycle was recorded.

Absorption values for each particle were determined after freeze-and-thaw testing. Each particle (or major piece) was dried to a constant weight at 230 F (110 C). The absorption of each particle was calculated from

$$w = 100(W_T - W_S)/W_S,$$

where w = absorption expressed as a percent, W_T = saturated surface-dry weight of particle (or major pieces), and W_S = oven-dry weight of particle (or major pieces). Porosity caluclations were made using

$$\eta = 100\ G_{SSD}w/(100 + w),$$

where η = porosity expressed as a percent and G_{SSD} = bulk specific gravity (saturated surface dry). It should be emphasized that the above equation applies only for saturated aggregates.

The accumulated number of fractured particles at the end of each freeze-thaw cycle, expressed as a percentage of the total number of particles, is presented graphically in Figure 5. The largest increase occurred at the end of the first cycle. Of the total number fractured, approximately 70 percent occurred during the first freezing cycle. The small increases in the accumulated percentage of fractured particles which occurred with succeeding cycles are probably due to the fact that many of the particles had undetected fractures at the end of the first freezing cycle, and additional cycles were needed before the fractures became visible.

The percentage of fractured particles at the end of the fourth cycle of freeze-and-thaw, for each particle size tested, is given in Figure 6. The largest percentage of fractured particles occurred in the 1/2-inch (12-mm) size; the smallest percentages occurred in the 1-inch (25-mm) and No. 4 sizes. The average percentage of fractured particles in all sizes combined was 53.6 percent. The 1-inch (25-mm) particles consisted mostly of igneous and metamorphic rock particles which, by their mode of formation, are less porous than water-lain sedimentary rocks. The bulk of the 1/2-inch (12-mm) particles consisted of porous cherts and porous dolomites. The bulk of the No. 4 particles was mostly quartz.

The relationship between soundness of the test particles and their adjusted porosity values is shown in Figure 7. As expected, particles in the higher porosity range were less durable than particles of the lower range. All particles having a porosity of more than 11 percent fractured in the freeze-thaw test; less than 25 percent of the particles having a porosity of less than two percent fractured.

A graph depicting the relationship between percentage of fractured particles and absorption values of test particles is also shown in Figure 7. All particles having absorptions of four percent or greater failed when subjected to freezing and thawing. Very few specimens having absorptions of less than one percent failed. Between these extremes, percentage of particles failing increased as absorption increased.

Theory

The ability of a rock fragment to withstand internal pressures accompanying freezing is controlled

by certain inherent properties of the fragment. Insight into these properties is gained from Timoshenko's explanation *(4)* of Lame's solution for the radial and tangential stresses in a thick-walled, spherical container under internal and external pressures. If the exterior confining pressure (P_o) is zero, Timoshenko's equation for radial stresses (σ_r) at the exterme outer fiber is

$$\sigma_r = 0.$$

For tangential stresses (σ_t), Timoshenko's equation reduces to

$$\sigma_T = 3P_i a^3/2(a^3 - b^3)$$

where P_i = internal pressure, a = inner radius of the sphere, and b = outer radius of the sphere. Substituting from $V_v = 4\pi a^3/3 = \eta V_t$ and $V_t = 4\pi b^3/3$, where V_v = volume of voids, V_t = total volume of sphere, and η = porosity = V_v/V_t, the equation for tangential stresses reduces to

$$\sigma_t = 3 P_i\eta/2(1 - \eta).$$

The radial stress, σ_r, along the outer edge of the spherical container is zero and the tangential normal stress, σ_t, at the same point, which is a tensile stress, is dependent upon the porosity and tensile strength of the container and is independent of size or total volume.

If the tensile strength, σ_u, is inserted in the above equation for σ_t, the equation becomes

$$P_u = 2 \sigma_u (1 - \sigma)/3\sigma,$$

where P_u = maximum allowable internal pressure and σ_u = tensile strength. Tensile strengths of the gravel particles were not determined, but similar materials have tensile strengths ranging from 100 to 1000 psi (0.7 to 7 MPa). With a known tensile strength, the maximum allowable internal pressure for various porosity values may be calculated. Three porosity-pressure curves for tensile strengths of 300, 600, and 900 psi (2, 4, and 6 MPa) are shown in Figure 8.

The determination of the internal pressure accompanying freezing of water within a hollow sphere may, likewise, be approached from a theoretical standpoint. If the temperature-volume changes of the sphere, water, and ice are neglected, the volume of ice (V_I) within the cavity, assuming all the water freezes, is as follows:

$$V_I = 4\pi a^3 S(1 + \beta) (1 - P_i K)/3$$

where S = degree of saturation, β = volume increase accompanying freezing of water, and K = bulk modulus of ice. The tangential strain at any point within the sphere is given by

$$\epsilon_t = \delta/r = (\sigma_t/E) - \mu(\sigma_r/E),$$

where ϵ_t = tangential strain, δ = radial displacement, E = Young's modulus of elasticity of the sphere, μ = Poisson's ratio of the sphere, and r = radial distance. Assuming $P_o = O$ and substituting for V_v and V_t, the increase in the radius of the internal cavity or void due to an internal pressure reduces to

$$\delta = aP_i (1 + \mu + 2\mu - 4\mu\eta)/ 2E(1 - \eta).$$

The volume of the cavity, V_c, under internal pressure will thus increase to

$$V_c = 4\pi a^3 (C^3P_i^3 + 3C^2P_i^2 + 3CP_i + 1)/3$$

where $C = 1 + \mu + 2\mu - 4\mu\eta)/ 2E (1 - \eta)$. The volume of the ice within the cavity must be equal to the volume of the cavity. By equating the two and rearranging, it follows that

$$P_i^3 + 3P_i^2/C + P_i (3CK + S + S\beta)/C^3K + (1 - S - S\beta)/C^3 = 0.$$

The internal pressure was calculated for various porosity values using the following values: μ = 0.365, E = 1.0 x 10^6 psi (6.9 GPa), K = 1.2 x 10^6 psi (8.3 GPa), S = 1.00, and β = 0.0917. This plot is superimposed on the maximum allowable internal pressure curves in Figure 8.

The intercepts between the maximum and available pressure curves are maximum safe porosity values. At porosities greater than these, the maximum available pressure is not needed to cause rupture. Pressure is dependent upon temperature; and so as porosity increases, less pressure -- and consequently less severe temperatures -- will cause failure. Figure 8 also shows the same theoretical relationship between disruptive temperature, porosity, and tensile strength. For a given tensile strength, the disruptive temperature increases as porosity increases, and it may be noted that rupture would occur at a temperature slightly below freezing if the porosity is high.

It appears that the range over which critical porosity occurs is a manifestation of the inherent tensile strength of the aggregate. Whereas it must be presumed that tensile strength varies in inverse proportion to porosity, the inherent tensile strength varies within a wide range depending on the mineralogical nature of the aggregate. Hence, the force opposing the expansion accompanying freezing -- and therefore the limiting pressure -- is governed by the restraining strength of the aggregate or the confining vessel. Logically, an encasement medium -- such as mortar or concrete -- will provide additional restraint against the forces emanating from a dilating particle of aggregate. Thus, restraint increases with depth of embedment. A saturated particle of aggregate in concrete may be viewed as being a center of compression, and the surrounding concrete may be viewed as a thick-walled shell or vessel. Of course, at near-surface locations, the restraint is unbalanced; and "pop-outs" or cracking will result if the dilating pressures are critical.

PRESSURES ASSOCIATED WITH POP-OUTS

Pop-outs and deep-seated deterioration are generally associated with high absorptivity and high saturation. Aggregate particles of all sizes are capable of inducing damaging pressures. Particles which

are near the surface may produce pop-outs even though the dilating pressures are relatively low -- the surrounding shell of concrete offers only minor restraint.

Phenomena

To gain a better understanding of the mechanisms associated with these signs of distress, failures were induced by subjecting voids of varying diameters and depths below the concrete surface to hydrostatic pressure *(5)*. Concrete specimens, 10 x 10 x 4 inches (254 x 254 x 102 mm) were cast from six-bag concrete containing limestone coarse and fine aggregates. The specimens were moist cured at 77 F (25 C) for 28 days prior to testing. Each specimen was then drilled with a flat-faced masonary bit to form a cylindrical hole in the center of a 10- x 10-inch (254- x 254-mm) surface. Hole depths for the various specimens ranged from 2-1/2 to 3-7/8 inches (63.5 to 93.4 mm) so as to provide depths of burial ranging from 1-1/2 to 1/8 inches (28.1 to 3.2 mm). The diameters of bits used for drilling the various specimens were 1/4, 3/8, 1/2, 3/4, 1, and 1-3/8 inch (6.4, 9.5, 12.7, 19.1, 25.4, and 34.9 mm). A 1/4-inch (6.4-mm) high-pressure tube and rubber gasket assembly was placed in each specimen to within 3/4 inch (19.1 mm) of the bottom of the void. The tubing and gasket were held in place with high-strength epoxy cement. In all cases, the void depth was 3/4 inch (19.1 mm), and only the void diameter and depth of burial were varied.

A hand-operated pump capable of producing a maximum pressure of 5000 psi (34 MPa) was connected to the pressure tubing, and glycerin was pumped into the artifical void at such a rate that the pressure zone was limited essentially to the pressure cavity. This method was later used by Bache and Isen *(6)* to illustrate failure patterns. The time required to attain the final pressure was approximately 10 seconds. Characteristics of resultant pop-outs are illustrated in Figure 9. Pressures required to produce pop-outs in the various specimens are shown by the series of curves in Figure 10. These curves present data obtained from tests on 150 specimens. Results obtained had a remarkably high degree of duplication. For similar depths of burial, greater pressures were required to produce pop-outs in the small diameter cavities than required for the larger cavities. Figure 10 indicates a cover of about 0.9 inch (23 mm) would be necessary for protection against failure from pressures expected within a 1/4-inch (6.4-mm) cavity, and a cover of approximately 1-1/4 inch (31.8 mm) would be needed for 1-3/8 inch cavities. All pop-outs were predominantly conical, and thinning was more pronounced along the outer surface perimeter of the larger pop-outs. Failure widths for the 3/4-inch and 1-inch cavities at varying depths of burial are shown in Figure 11. Failure angles were computed from the fitted curves and are plotted in Figure 12. The failure angle is significantly related to cavity diameter and depth of burial.

Specimens containing cavities which were more deeply buried split into two sections as depicted

in the sketch inserted in Figure 13. Pressures required to produce this type failure varied with cavity diameter but were independent of depth of burial -- that is, above the limit of pop-out failure. Pressures to induce failures of this type should not vary appreciably with depth of burial since the area of resistance to failure was constant (4 x 10 inches (102 x 254 mm)) for all specimens. The limiting depth of burial for a given cavity diameter at which the mode of failure changes is naturally governed by specimen dimensions, and pop-outs would occur at greater depths of burial in specimens of larger sizes than those tested in the series reported herein. Splitting-type failures are represented on the curves in Figure 10 in the zones of zero slope. Failures of this type may be considered as deep-seated deterioration commonly associated with deeply embedded and highly absorptive aggregate particles. High dilating pressures are necessary for these failures since the particles are more restrained.

Additional tests were conducted by casting water-filled spherical capsules in concrete specimens of the same size as previously tested. A copper-constantan thermocouple was placed in the center of each sphere of water, and voltages were amplified and recorded. Temperature measurements within 1/4 C were possible with this arrangement. Pressures accompanying confined freezing of water within the spheres were computed from the temperature data. The temperature at failure was 24 F (-4.0 C) with an accompanying pressure of 7200 psi (50 MPa). Following rupture, the pressure subsided and the freezing point returned to normal. Freezing thereafter was isothermal. These events were displayed over a series of successive cycles rather than within a single temperature excursion. This was interpreted as a manifestation of progressive damage.

Theory

Within a semi-infinite mass, there is a free-field stress distribution. When the continuity of an "assumed" homogeneous material such as concrete is interrupted by the presence of a porous and saturated aggregate particle undergoing freezing, stresses near the particle are no longer equal to the free-field stresses since a discontinuity of strains or deformations occur at the aggregate-matrix interface. Because of this discontinuity, the induced differential pressures alter the at-rest stress conditions that existed prior to freezing. Shear stresses are therefore mobilized within the concrete matrix; and, if the shearing strength of the concrete is exceeded, the material may fail in the form of a pop-out.

When a freezing aggregate particle is contained in a concrete mass, relative displacements between the particle and the surrounding matrix will occur. As a result, shearing stresses will be mobilized along those planes which experience shearing distortions. Because of the extremely high pressures which sometimes are developed in freezing aggregate particles, the modulus of the porous particle may be assumed to be greater than that of the surrounding concrete matrix. The conditions which result may be, in

a general way, assumed to be analogous to the phenomenom of stress transference called "passive arching".

The application of theoretical solutions implies that the material behaves elastically. It is known that such behavior may depart from ideal elasticity under the high pressures obtained. However, elastic solutions are good approximations when small displacements are involved. At large displacements, the stresses in certain regions reach the yield stress, and the stress distribution that finally results may be quite different from the stress distribution determined by considering only elastic equilibrium. Immediately above plane CD in Figure 14, movement of the concrete matrix is denoted by arrows E and F. The material just above CD tends to move upward as a result of the high pressures induced by freezing and expanding water within the aggregate. The material to the sides of the aggregate particle thus tends to move laterally, creating a condition analogous to the passive pressure state. If deformations proceed far enough and the depth of burial is sufficiently small, the failure surface may propagate to the surface of the concrete mass and result in a pop-out failure. The lateral stresses which occur at the limiting stage of lateral compression are called passive pressures. Rankine's theory gives the passive pressure as

$$P_P = \gamma d \tan^2 (45^\circ + \phi/2) + 2c \tan (45^\circ + \phi/2),$$

where P_P = passive pressure, γ = unit weight, d = depth of burial, c = cohesion, and ϕ = angle of friction. Using typical values of 150 pounds per cubic foot (2.4 Mg/m^3) for the unit weight of concrete, cohesion of 950 psi (7.8 MPa), and a friction angle of 47°, the passive pressures calculated from the above equation are in the order of 4800 psi (33 MPa). It is interesting to note, since the depth of burial is small, that the term in the above equation involving the depth is extremely insignificant. It is also interesting to note that the passive pressures obtained from the above equation are on the same order of magnitude as the compressive strength of the concrete.

In Figure 14, assuming passive pressures act over a rectangular surface with dimensions equal to the depth of burial and the void diameter (perpendicular to the plane of the figure), passive forces can be calculated. Assuming a coefficient of passive pressure of 3, the forces acting at the top interface between the void and the concrete value of the void pressure can be obtained. Table 1 summarizes such calculations for the range of the depth of burial and the void diameter sizes investigated. It is interesting to note the remarkable agreement between calculated void pressures and void pressures observed to cause pop-out failure. Comparison of the calculated and observed values is extremely satisfactory in all except one case, the 1-inch (25.4-mm) depth of burial for a void diameter of 1/4 inch (6.4 mm).

On the basis of the few calculations presented in the Table 1, it seems reasonable to consider the passive pressure concept as being adequate in explaining the mode of failure for pop-outs. In the case of the 1/4-inch (6.4-mm) diameter void buried 1 inch (25.4 mm) beneath the surface, the mode of failure may be different; thus, pressures originating at depths of three or four or more times the cavity

size cannot significantly exceed the compressive strength of the concrete.

SUMMARY AND CONCLUSIONS

It has been demonstrated that aggregates having an absorption greater than four percent are likely to rupture upon freezing; aggregates having an absorption less than one percent are generally unaffected by freeze-thaw. A composite sample of aggregate particles may, collectively, absorb less than four percent water by weight and still contain individual particles having absorptions significantly greater. Absorption tests based solely on composite samples are not adequate in this respect. Degradation of composite samples subjected to saturation and quick freezing cycles could provide a measure of the proportions of sound and unsound particles. Alternatively, each particle within a composite sample may be tested for absorption; and the proportions of deleterious material may then be resolved statistically.

Concretes may contain as much as 20 percent voids. Theoretically, the critical volume of water in a vessel is 91.7 percent of saturation (capacity). It is intuitively apparent that the system of voids within a mass of concrete is infinitely complex. It would be possible, therefore, for certain cavities or pores to be critically saturated while others may be relatively unsaturated. Here again, gross absorption alone fails to define the state of saturation -- that is, unless saturation is complete in all respects. Forced saturation renders concretes and(or) aggregates susceptible to damage through freezing. The entrainment of air, evidently, causes concrete to be infinitely more difficult to saturate -- probably due to disconnection of the voids and(or) the back-pressure of air in minute spherical voids. Aggregate particles are usually not "immunized" in this way and tend to saturate preferentially. Nevertheless, it seems reasonable to conclude that any mechanism whereby saturation is delayed or rendered improbable enhances the welfare or durability of concrete exposed to freezing weather.

REFERENCES

1. Dorsey, N. E., **Properties of Ordinary Water-Substance**, Reinhold Publishing Co., New York, 1940.
2. Havens, J. H., *Thermal Analysis of the Freeze-Thaw Mechanism in Concrete*, **Bulletin No. 59**, Engineering Experiment Station, University of Kentucky, 1961.
3. Scott, J. W. and Laughlin, G. R., *A Study of the Effects of Quick Freezing on Saturated Fragments of Rocks*, Division of Research, Kentucky Department of Highways, February 1964.

4. Timoshenko, S., **Theory of Elasticity**, McGraw-Hill Book Co., Inc., New York, 1934.

5. Scott, J. W., Laughlin, G. R. and Havens, J. H., *Freeze-and-Thaw Characteristics of Aggregates,* Proceedings of the 16th Annual Highway Geology Symposium, **Bulletin No. 76**, Engineering Experiment Station, University of Kentucky, September 1964.

6. Bache, H. H. and Isen, J. C., *Modal Determination of Concrete Resistance to Popout Formations,* **Journal**, American Concrete Institute, June 1968.

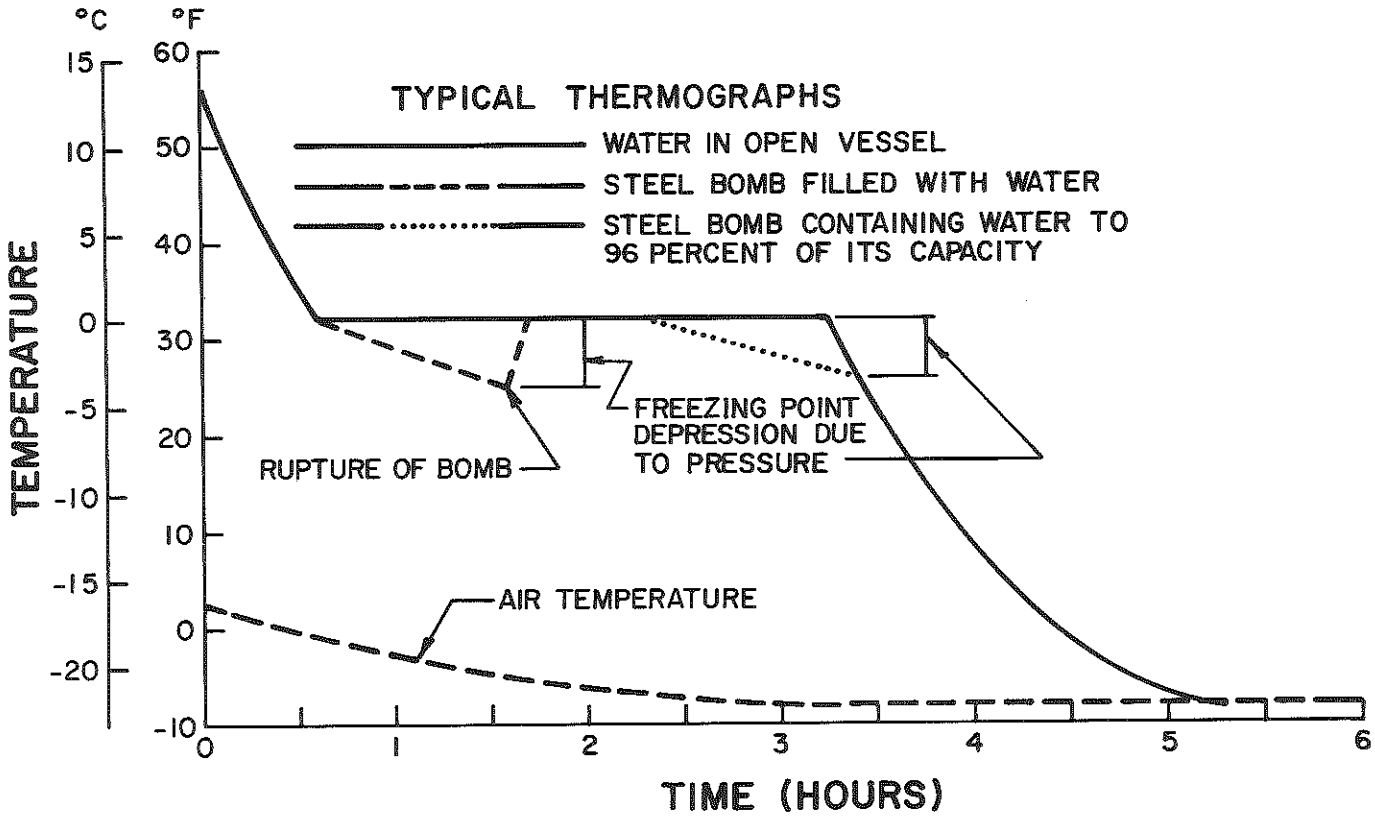

Figure 1. Typical Thermographs.

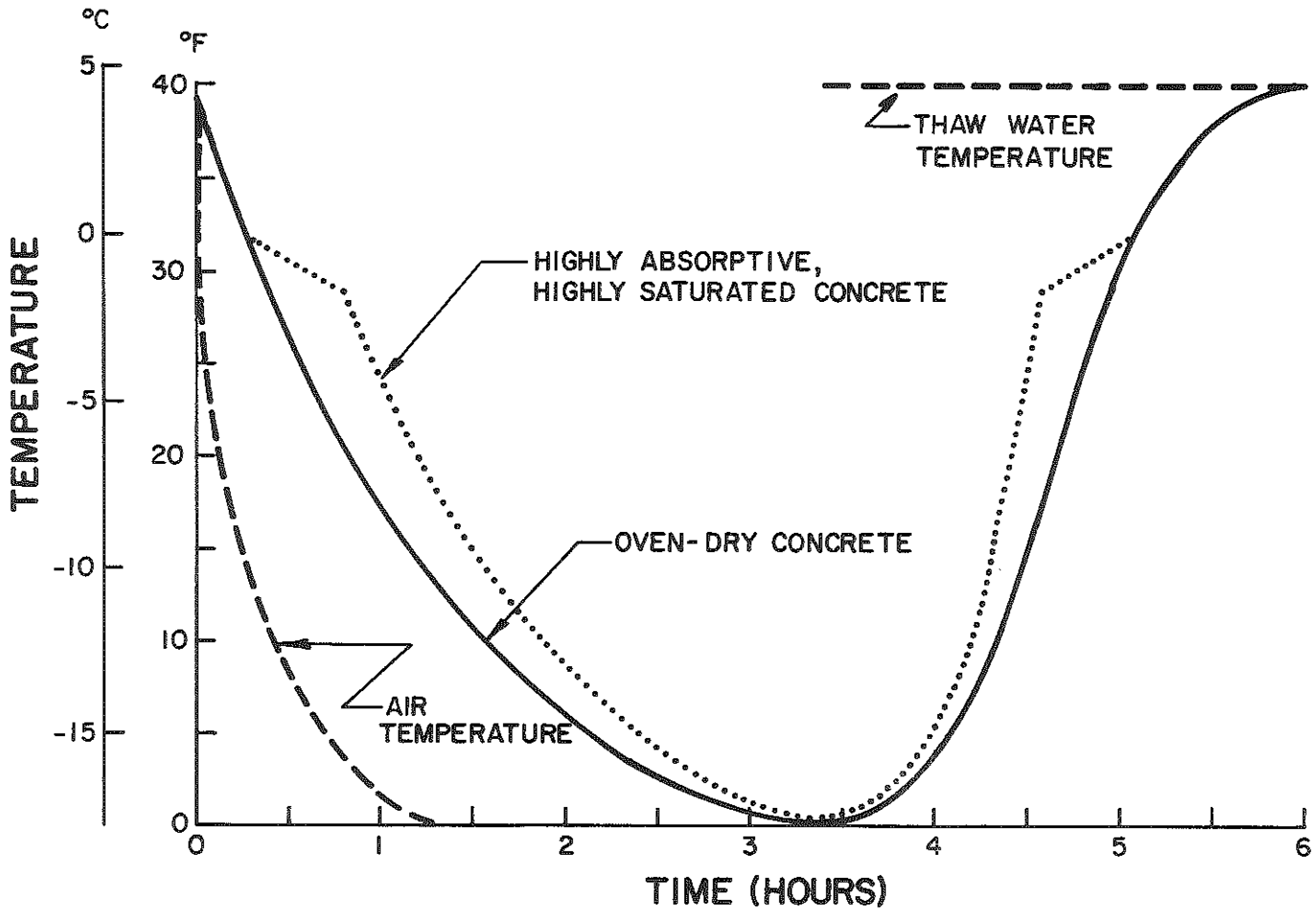

Figure 2. Typical Time-Temperature Records Obtained from Concrete Undergoing a Single Cycle of Freeze-Thaw.

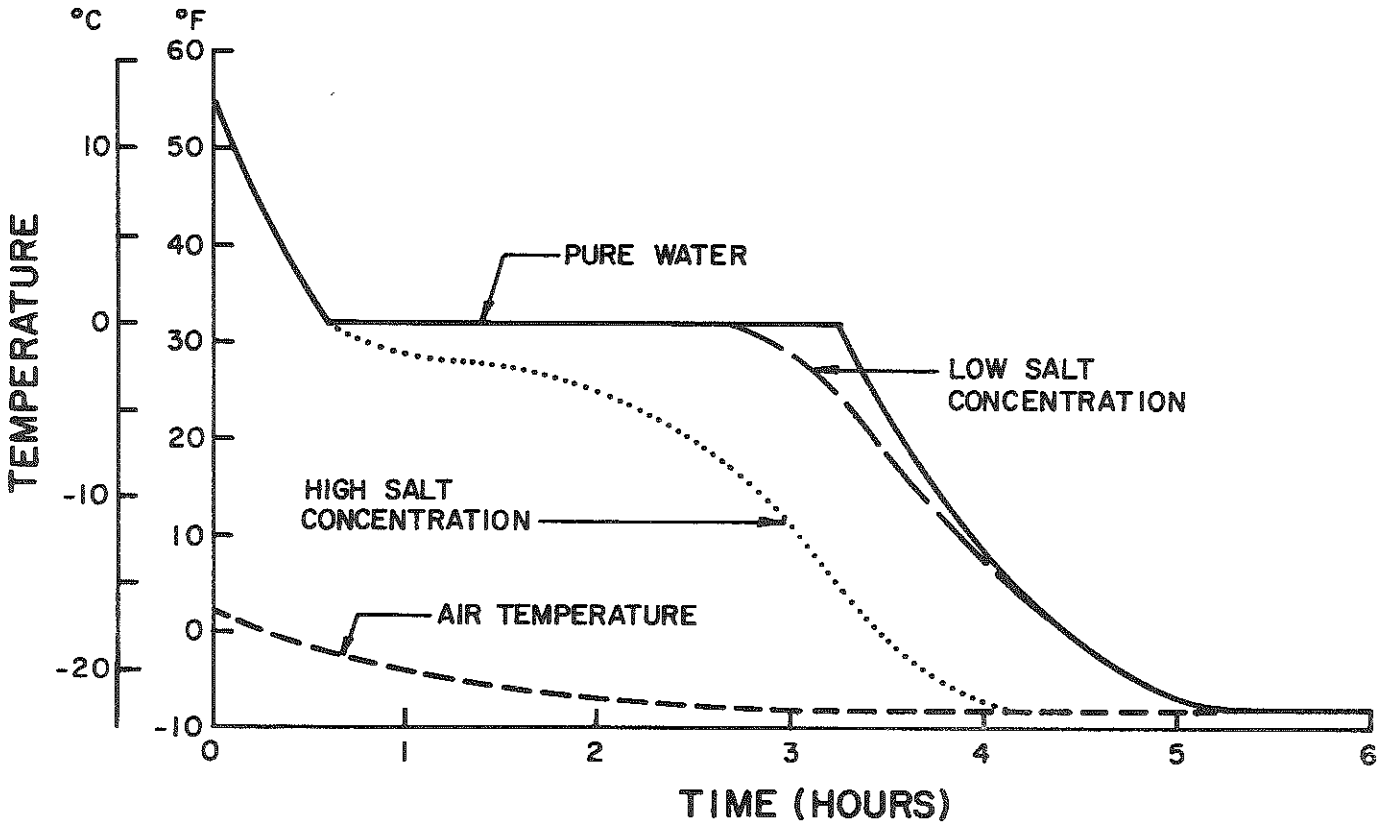

Figure 3. Probable Effects of Solute upon the Time-Cooling Curve.

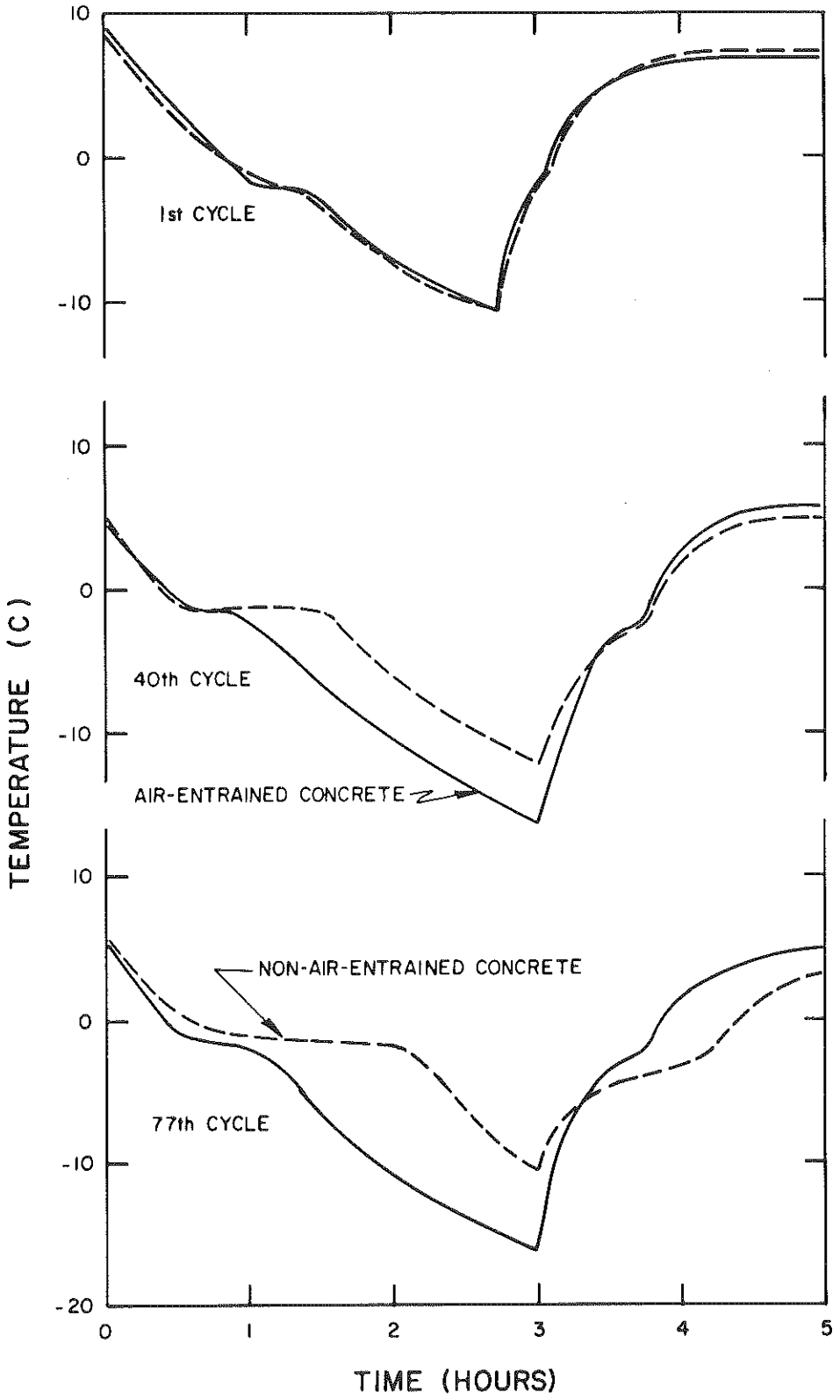

Figure 4. Time-Temperature Records from Concrete Containing 0.7 and 13 Percent Air; Moist-Cured 14 Days; Soaked 24 Hours.

Figure 5. Accumulative Percentage of Fractured Particles for Each Cycle of Freeze-Thaw.

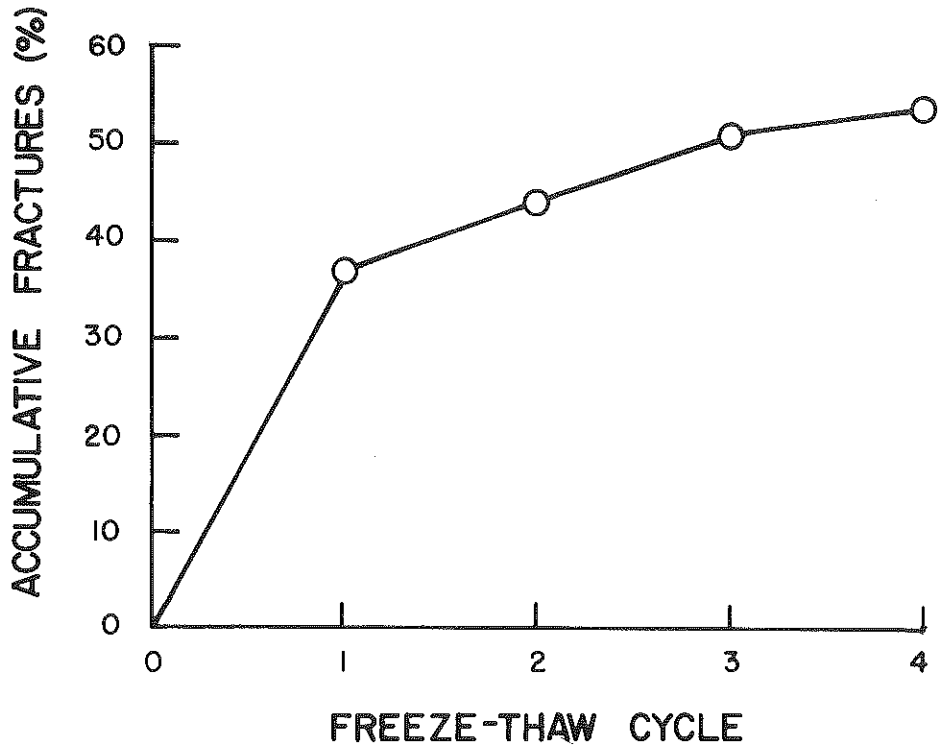

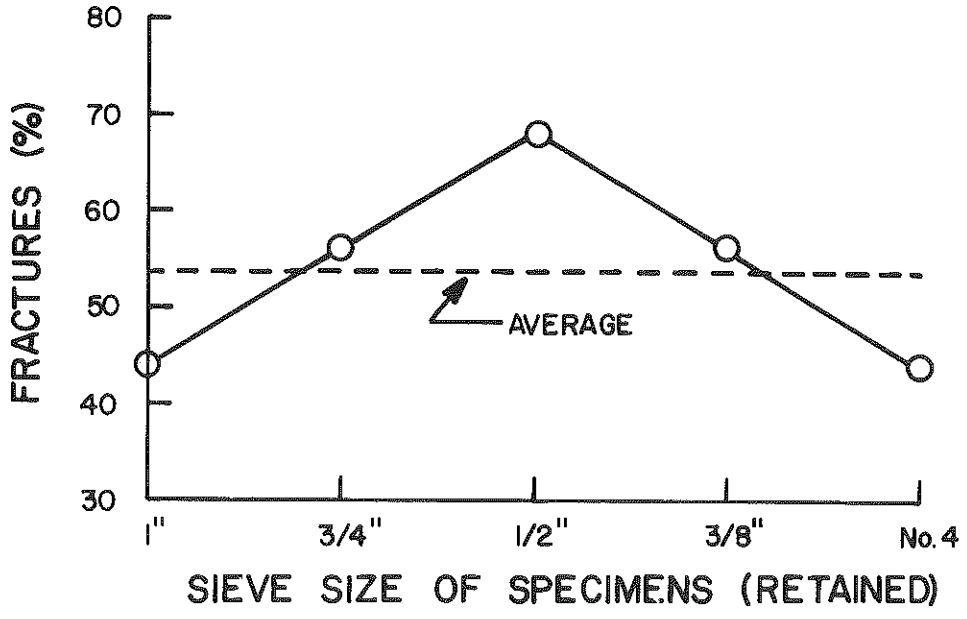

Figure 6. Relationship between Particle Size and Percentage of Fractured Particles after Exposure to Four Cycles of Freeze-Thaw.

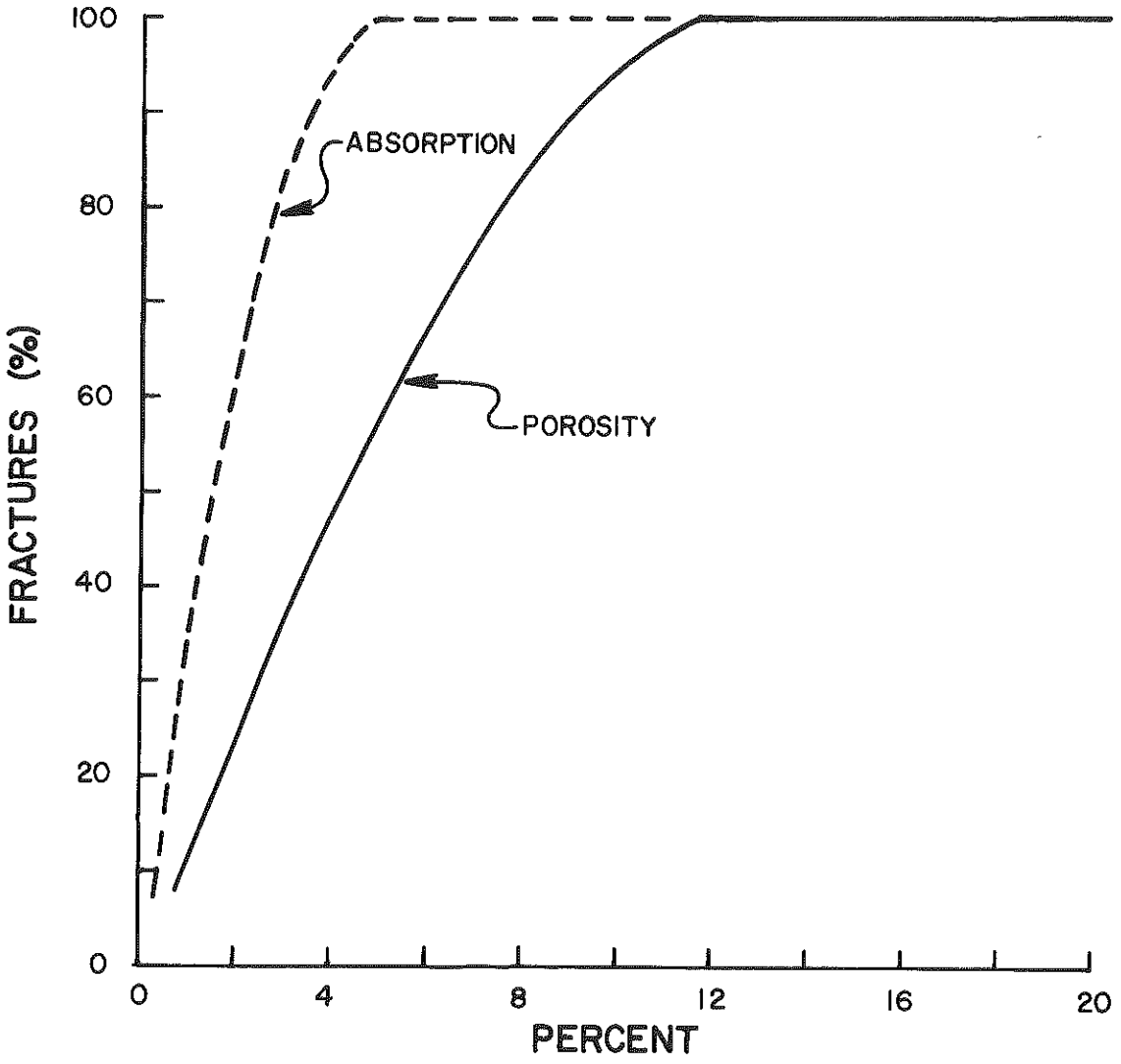

Figure 7. **Relationship between Porosity and Absorption and Percentage of Fractured Particles after Exposure to Four Freeze-Thaw Cycles.**

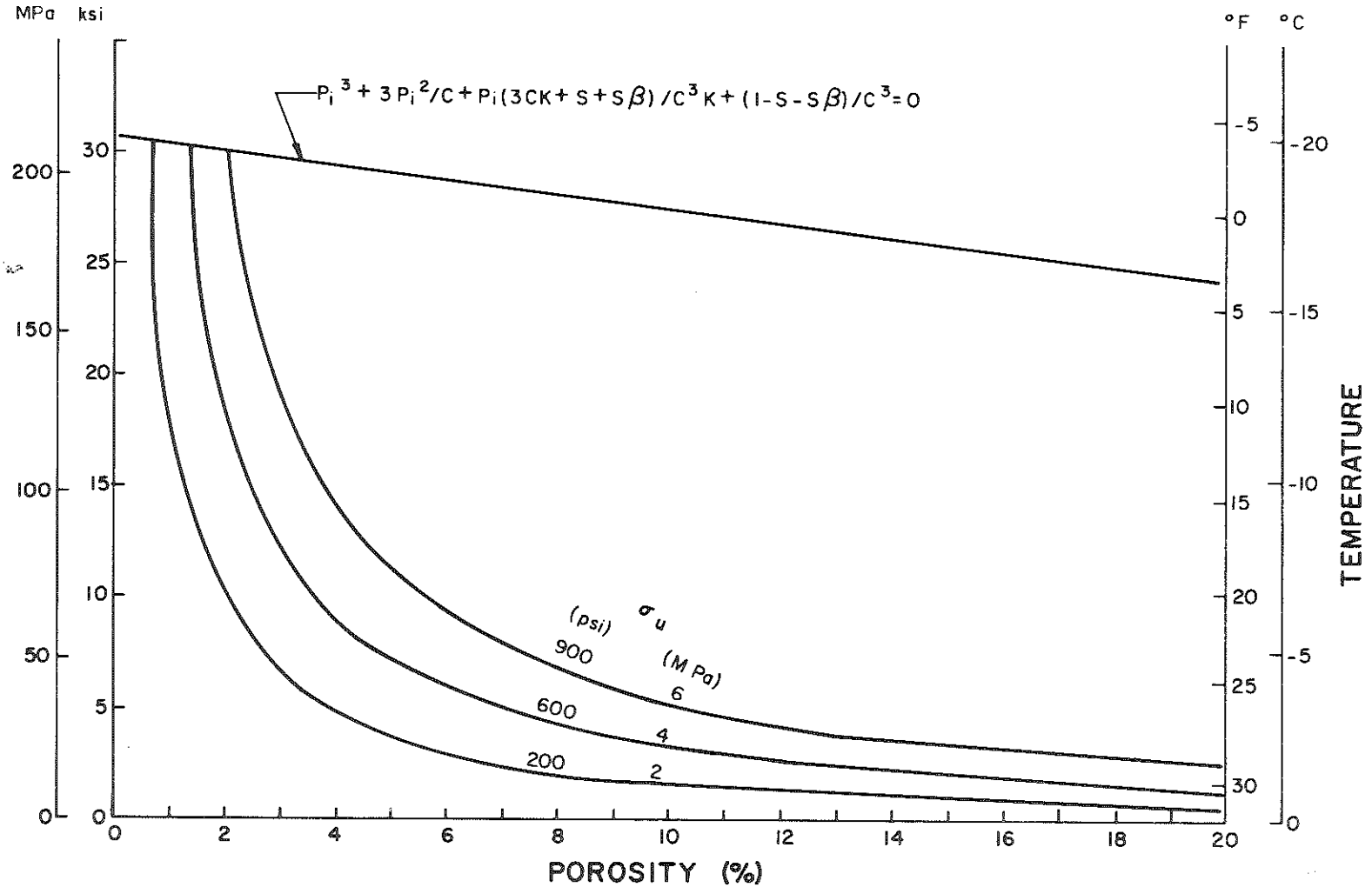

Figure 8. Suggested Theoretical Relationships for Varying Tensile Strengths.

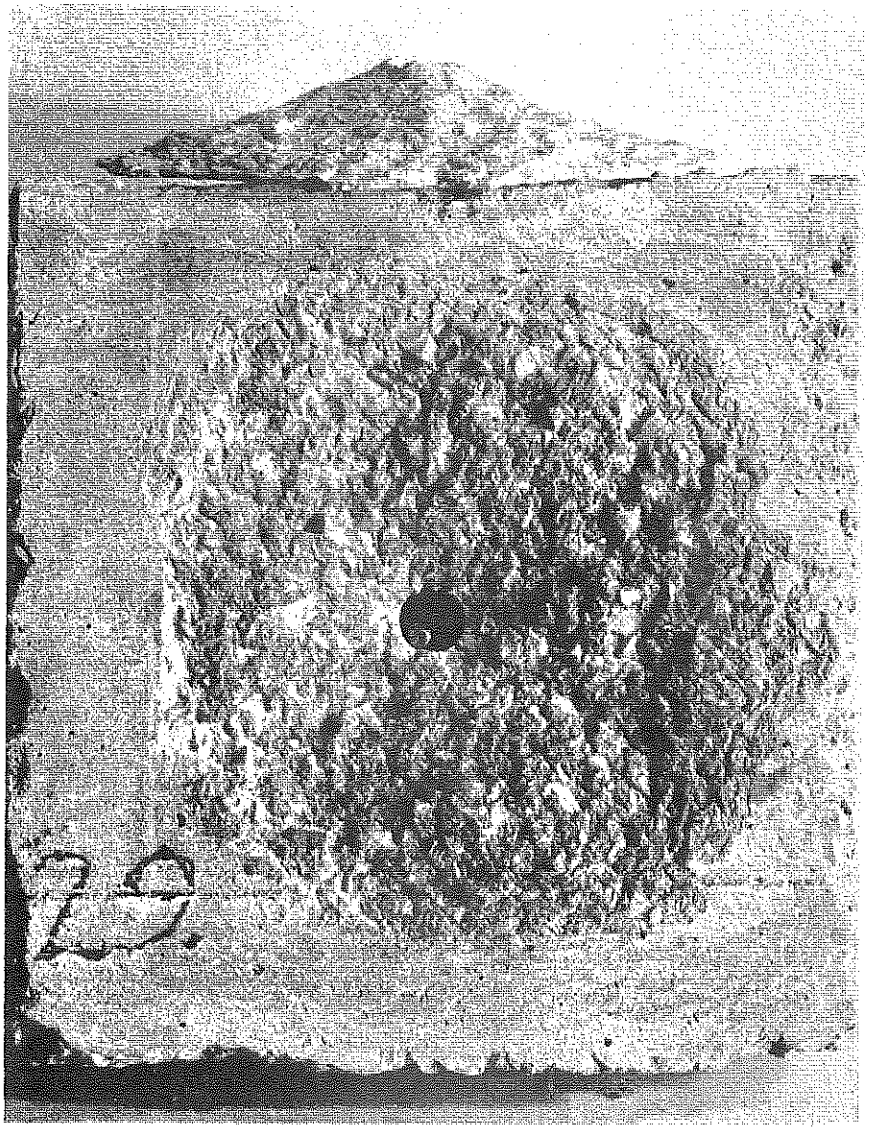

Figure 9. Photograph of Test Specimen Showing Pop-Out.

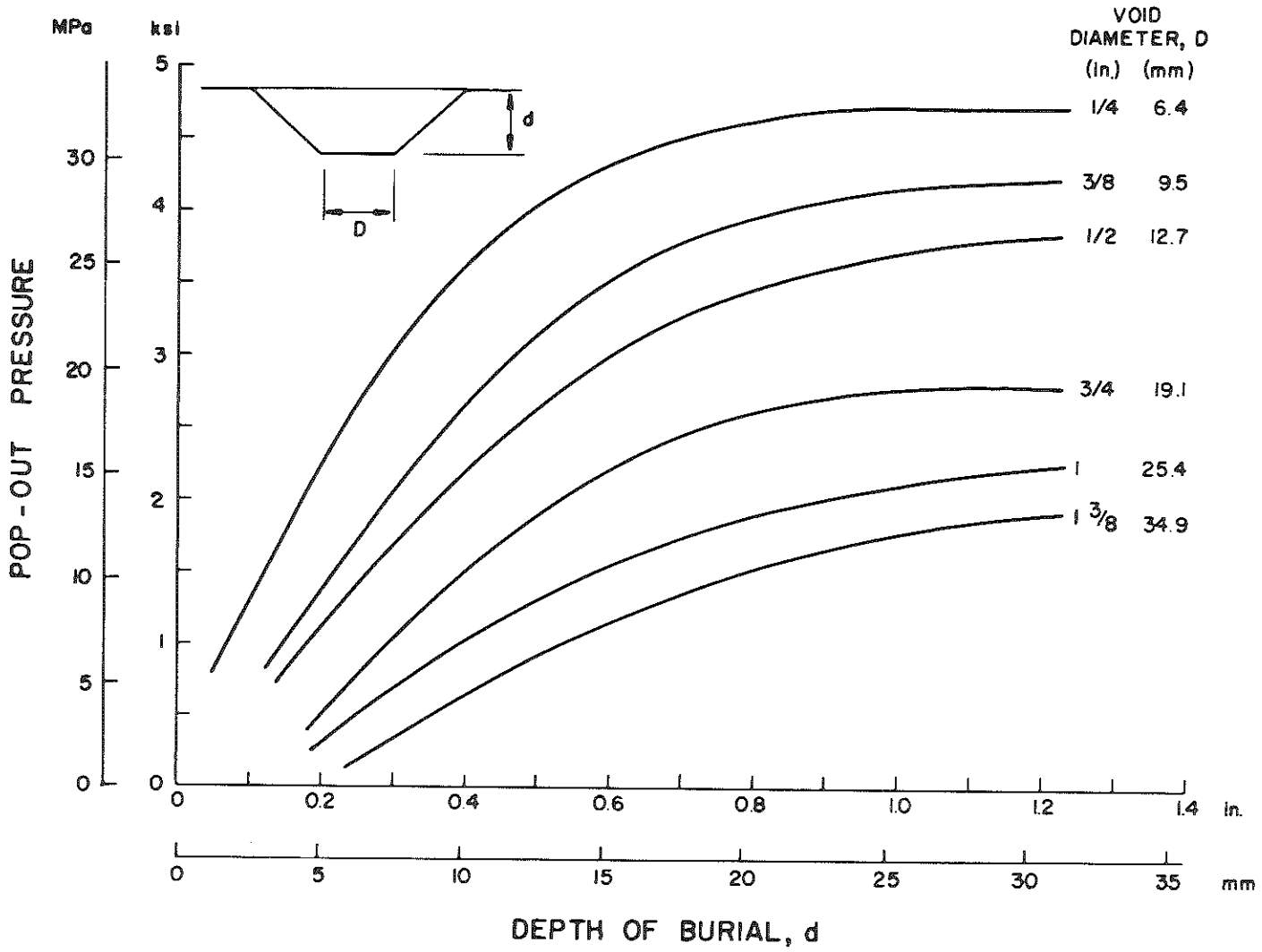

Figure 10. Relationship between Pop-Out Pressure, Void Diameter, and Depth of Burial.

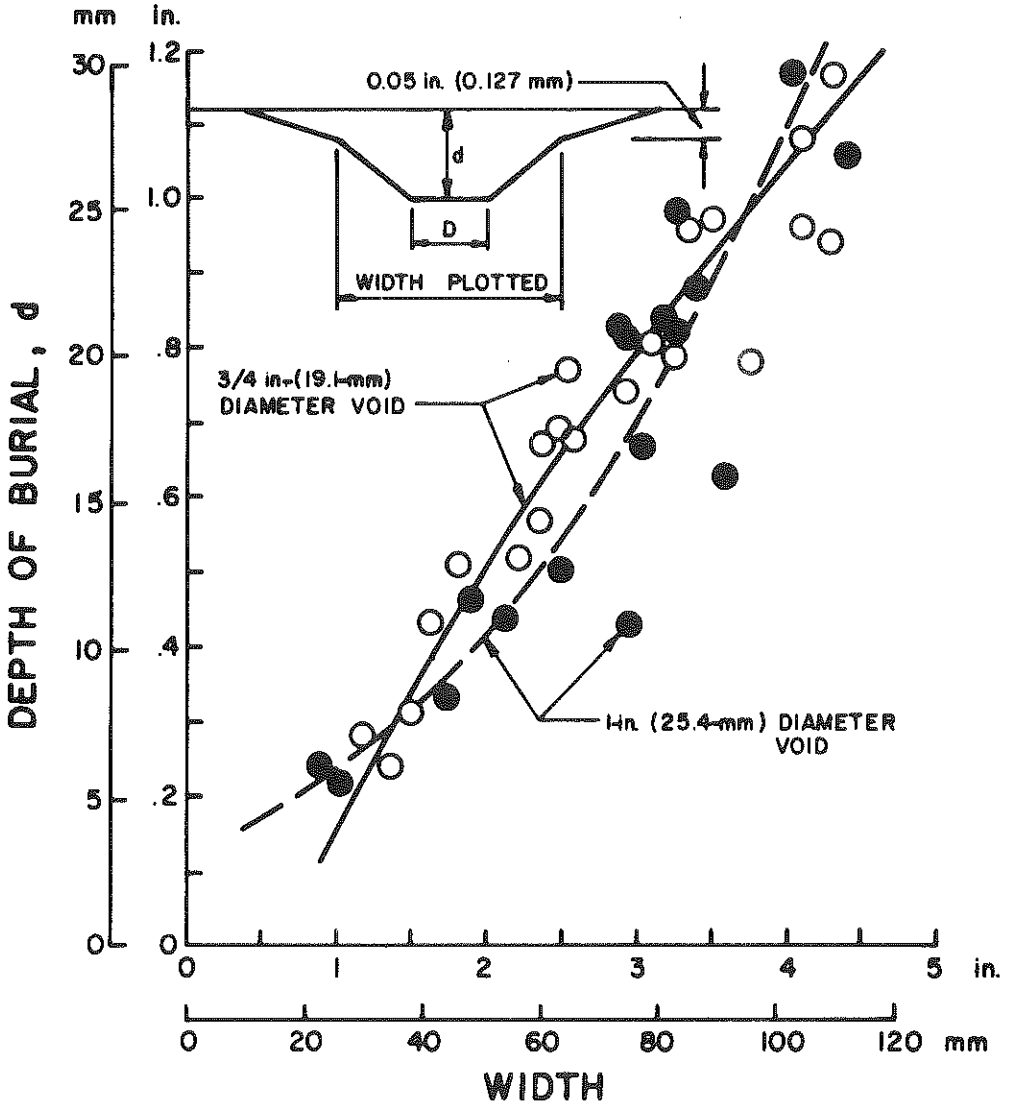

Figure 11. Relationship between Depth of Burial, Void Diameter, and Pop-Out Width.

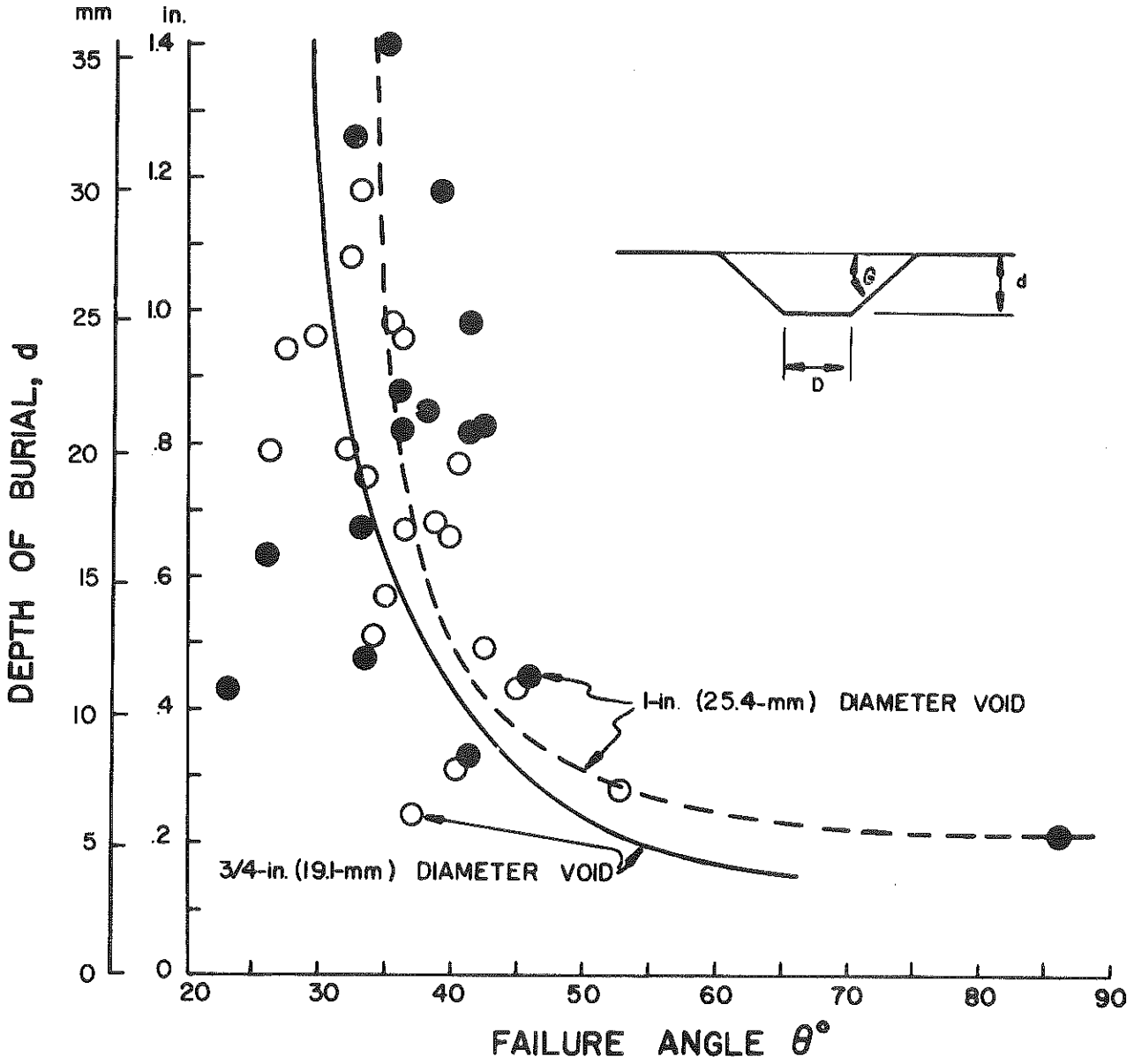

Figure 12. Relationship between Failure Angle and Depth.

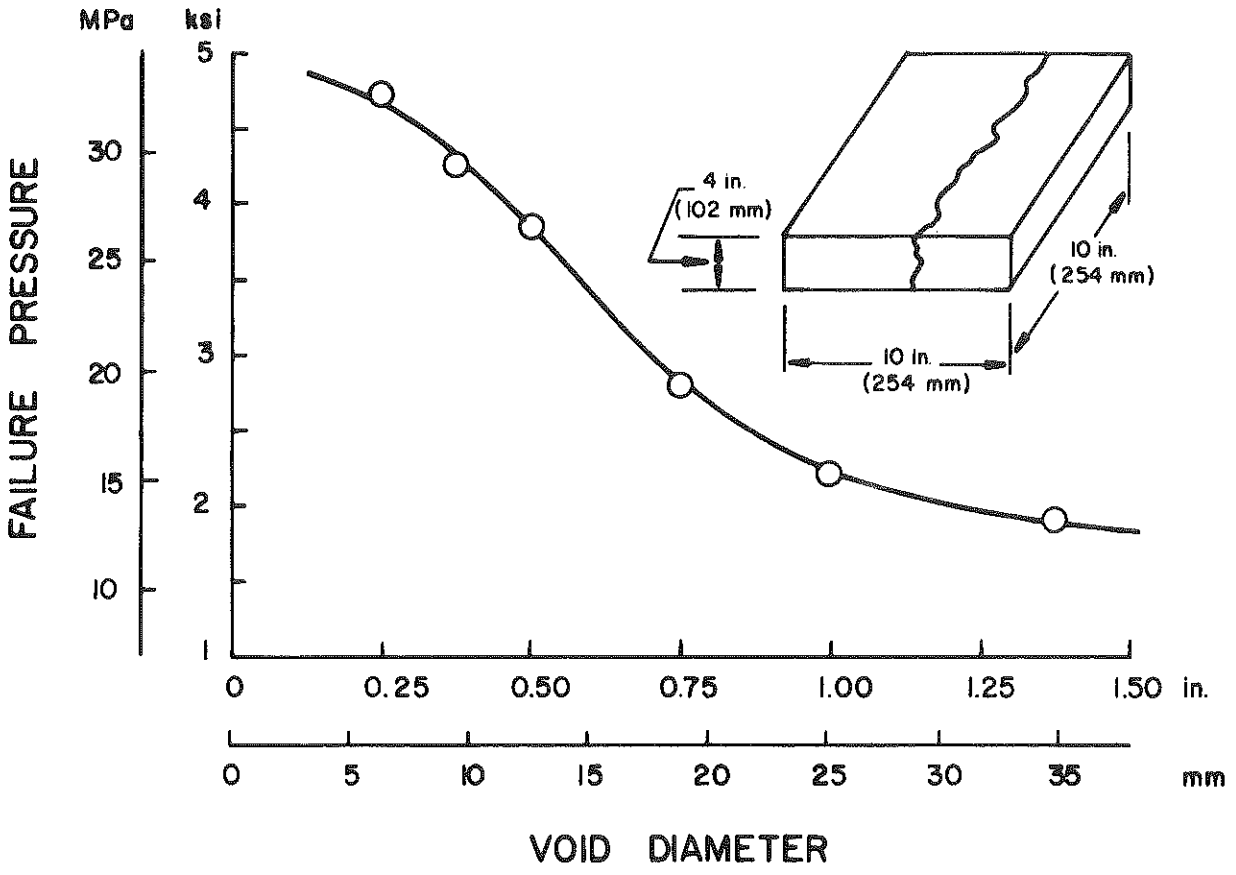

Figure 13. Pressure Necessary to Produce Splitting Failure in Deeply Buried Voids.

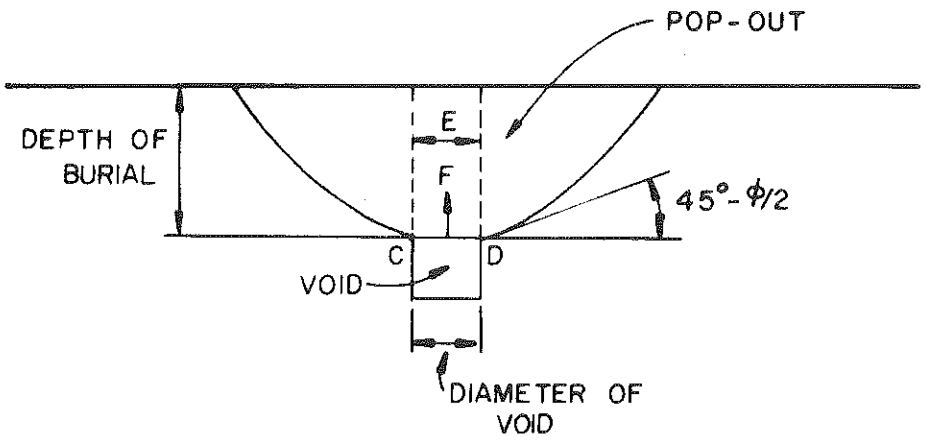

Figure 14. Passive Pressures and Pop-Outs.

TABLE 1. PASSIVE PRESSURES AND POP-OUTS

DEPTH OF BURIAL		VOID DIAMETER		VOID PRESSURE			
				CALCULATED		OBSERVED	
(in.)	(mm)	(in.)	(mm)	(psi	(MPa)	(psi)	(MPa)
1 1/2	38	1	25	2040	14.1	2150	14.8
1	25	1	25	1020	7.0	1300	9.0
1 1/2	38	1 3/8	35	1465	10.1	1800	8.7
1	25	1 3/8	35	732	5.0	950	6.6
1 1/2	38	1/4	6	7850	54.1	4700	32.4
1	25	1/4	6	3925	27.1	4050	27.9